



Synthesis, structural elucidation and antiradical activity of a copper (II) naringenin complex

Gustavo Celiz · Sebastián A. Suarez · Analía Arias · José Molina · Carlos D. Brondino · Fabio Doctorovich

Received: 21 August 2018 / Accepted: 9 March 2019
© Springer Nature B.V. 2019

Abstract Coupling the extraction and derivatization of flavonoids to the *Citrus* processing industry is attractive from both the environmental and economic points of view. In the present work, the flavonoid naringin, obtained by “green” extraction with a water:ethanol mixture from waste grapefruit industry, was hydrolyzed to obtain naringenin. This flavonoid was used to synthesize the complex *trans*-di(aqua) bis(7-hydroxy-2-(4-hydroxyphenyl)-4-oxo-5-chromanolato) copper (II). This compound was characterized by spectroscopic techniques (UV/Vis, IR, Raman,

NMR and EPR), and by thermal analysis (TG and DSC). Then, a monocrystal of the complex obtained by dissolution and recrystallization in DMF was analyzed by single crystal X-ray diffraction. This is the first report of the crystal structure of a *Citrus* flavonoid complex. Additionally, its antiradical activity against 2,2-diphenyl-1-picrylhydrazyl (DPPH) was determined and compared with that for naringenin, demonstrating that coordination to copper enhances the antiradical activity of naringenin. According to the Mulliken population analysis conducted, by copper favors the delocalization and stabilization of the produced radical, since it acts as an electronic density acceptor.

Electronic supplementary material The online version of this article (<https://doi.org/10.1007/s10534-019-00187-3>) contains supplementary material, which is available to authorized users.

G. Celiz (✉)
Instituto de Investigaciones para la Industria Química (INQUI) and Universidad Nacional de Salta, Avenida Bolivia 5150, A4408FVY Salta, Argentina
e-mail: gceliz@unsa.edu.ar

G. Celiz · A. Arias · J. Molina
Facultad de Ciencias Exactas, Universidad Nacional de Salta, Avenida Bolivia 5150, A4408FVY Salta, Argentina

S. A. Suarez · F. Doctorovich
INQUIMAE, CONICET, Departamento de Química Inorgánica, Analítica y Química Física, Facultad de Ciencias Exactas y Naturales, Universidad de Buenos Aires, Pabellón II – Ciudad Universitaria - Núñez, C1428EHA CABA, Argentina

C. D. Brondino
Departamento de Física, Facultad de Bioquímica y Ciencias Biológicas, Universidad Nacional del Litoral/ CONICET, S3000ZAA Santa Fe, Argentina

Keywords Naringenin · *Citrus* flavonoids · Processing waste · Metal flavonoid complex · Crystallography

Introduction

Flavonoids are natural polyphenols that have a structure of benzo- γ -pyrone (C6–C3–C6). More than 8000 compounds with this skeleton have been identified, which are differentiated by various combinations of substituents, such as hydroxyls, methoxyls and *O*-glycosides. They are exclusive compounds of the plant kingdom, but species of the animal kingdom can obtain this polyphenols by eating, for example, cereals, fruits, and vegetables.

Among the different subclasses of flavonoids, flavanones occur mainly in *Citrus*. These compounds support and enhance the body's defenses against oxidative stress and help the organism in the prevention of cardiovascular diseases, atherosclerosis, and cancer (Barreca et al. 2017). Naringenin (Fig. 1) is a flavanone that occurs in low concentrations in *Citrus* fruits (Erlund 2004), but it can be obtained in large quantity by hydrolysis of naringin (Pulley 1936), a flavonoid that can be extracted easily from the solid waste generated in the industrial grapefruit production (Poore 1934).

Naringenin has biological action on humans. It could be useful in the treatments of osteoporosis (Swarnkar et al. 2012), some cancer type (Patel et al.

2014) and cardiovascular illnesses (Ilkay et al. 2015). These *in vivo* biological activities are due to its ability to interact with cell membranes (Selvaraj et al. 2014b), to quench radicals (Cavia-Saiz et al. 2010), to chelate transition metals that take part on radical production (de Souza and De Giovanni 2004) and interact specifically in various biological processes.

Among the great variety of flavonoid properties, the most studied has been the antioxidant activity. This activity is based on the ability of a substance to reduce the formation of free radicals, and to decompose those that are formed. The reason why antioxidant activity deserves interest lies in the fact that free radicals induce oxidative damage in biomolecules and organelles, which according to several studies may lead to diseases such as Parkinson's disease, heart disease and even cancer (Klein and Ackerman 2003; Smith et al. 2000; Valko et al. 2006; Waris and Ahsan 2006). Naringenin is not structurally favored to act as antiradical, because it does not possess the structural requirements that favor such activity: (i) ortho-dihydroxy substitution in ring B, which allows electronic delocalization in the radical products; (ii) conjugated double bond C2=C3 with group C4=O in ring C, which results in greater electronic delocalization in ring B; (iii) hydroxyl groups in positions 3 and 5, which can form hydrogen bonding with the group C4=O (Amic et al. 2007).

Chelation with metals alters the naringenin electronic distribution and this will cause changes in its spectroscopic, physicochemical, and certainly also biological properties. For that, it is interesting to

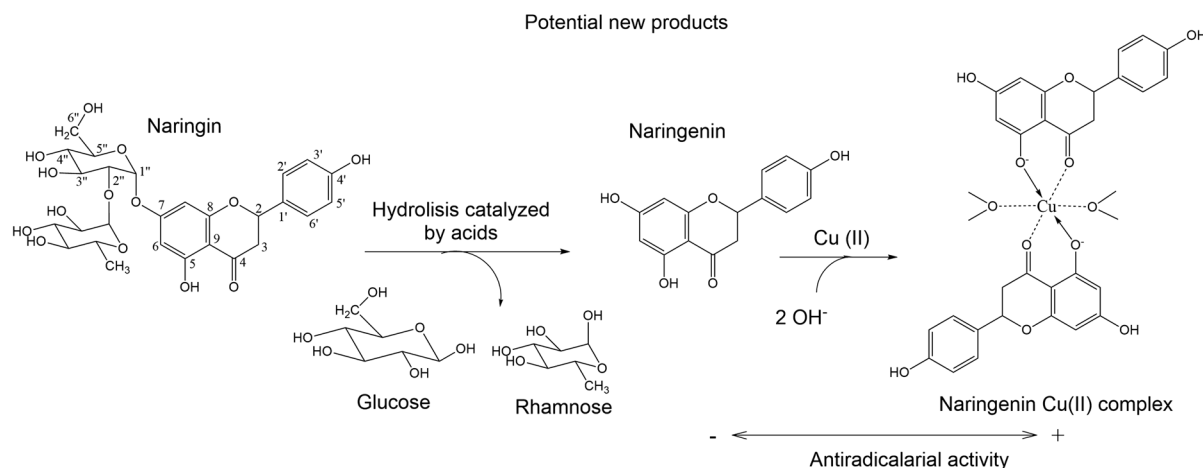


Fig. 1 Scheme of the synthesis of the naringenin Cu(II) complex starting from naringin

synthesize metal-naringenin complexes and study their properties to determine how the metal affects to the flavonoid. In order to study if the naringenin antiradical activity can be increased by complexation to a metal center, the synthesis of a complex of this flavonoid was proposed. Among the candidate metals, copper is a good choice, since it is a redox active metal, biologically relevant, and biocompatible. In addition, nowadays there are discrepancies among the different reports with regard to the structural and spectroscopic characterizations of the product obtained when naringenin and copper (II) react. This is probably due to the fact that complexes with different molar ratios and deprotonation states can be obtained in the synthesis (Brodowska 2013). Moreover, up to the moment, there is no report of the crystalline structure for any metal–*Citrus* flavonoid complex. For those reasons, the experimental data presented is focused on the characterization of the complex obtained, and on the radical scavenging properties of both naringenin and its Cu(II) complex.

This work presents the synthesis, purification and characterization of a complex formed between copper (II) and naringenin (Fig. 1). Spectroscopic properties (UV–VIS, IR, NMR, RAMAN), thermal analysis and a single-crystal X-ray diffraction study is presented to elucidate the three-dimensional structure of this complex. Additionally, an experimental and theoretical study about the radical scavenging activity of the complex and naringenin is presented.

Materials and methods

Materials

Naringin was produced from agro-industrial grapefruit waste using a simple and inexpensive process. It consists, briefly, on grinding the solid waste to an average size of 2–4 mm and, after that, performing an extraction in a fixed bed column with distilled water at 80 °C. Then, the extract obtained is cooled down, leading to crystallization of the flavanone. The precipitate was filtered, washed and, finally, dried at 50 °C.

Naringenin (NGE) was obtained from naringin by acid hydrolysis, using a reported method (Robin et al. 2007). Briefly, the process consists on hydrolyzing a 10% (w/v) aqueous solution of naringin with sulfuric

acid at 0.8 M concentration, stirring during 2 h at 90 °C. After that, the reaction media was cooled down to 4 °C, allowing the naringenin precipitation. It was then washed with cool water and dried at 50 °C. This process was done for a second time to ensure a complete conversion.

1,1-Diphenyl-2-picrylhydrazyl radical (DPPH) was purchased from Sigma (USA). All other reagents were of analytical grade.

Synthesis and purification of the copper (II) naringenin complex

A 25 mM solution of naringenin (272.3 g mol^{-1}) in ethanol:water solution (1:1) and a solution of copper (II) acetate at the same concentration in water were prepared. Both solutions were adjusted to pH 7 prior to the reaction. In order to have a 1:2 (metal:flavonoid) reactant stoichiometry, 100 mL of the naringenin solution were stirred and heated at 60 °C, and then 50 mL of copper salt solution was added dropwise. After the addition of the copper solution, the pH of the reaction mixture fell down to 6, so it was adjusted to pH 7–8 again. The reaction media was kept 1 h at 60–65 °C. After that, it was cooled overnight and filtered through standard filter paper. The solid obtained was washed first with ethanol:water 1:1 solution and then with acetone, to eliminate reactant traces (the complex was insoluble in these solvents). After that, it was filtered again, dried and stored at room temperature. The synthesized complex shows an apple-green color, instead of the pale-white color of naringenin. The obtained mass of purified complex was 0.7590 g, (yield = 95%).

Microanalysis experimental and calculated (in brackets) for $[\text{Cu}(\text{NGE})_2(\text{H}_2\text{O})_2]$: C: 56.3% (56.1%) H: 3.8 (4.0) %. Reinforcing this result, the same molar ratio metal:ligand, i.e. 1:2, was obtained by the Job's method (experimental details and results are provided in Supplementary Material). ESI Mass Spectrum, molecular ion: 411.98,568 m/z, expected for $[\text{Cu}(\text{NGE}(\text{H}_2\text{O})_3\text{Na})]^+$: 411.898563. In addition, the product was characterized according to the following sections.

Spectroscopic characterization

UV–Visible spectra (190–1100 nm) of naringenin and of the copper (II) naringenin complex were obtained in

dimethylformamide (at two concentrations) and water. Spectra in water were performed by adding 20 μL of flavonoid dissolved in DMF to 3980 μL of water. Spectra in solid state were carried out using a quartz cuvette for solids. The equipment used was a UV/Vis double beam spectrophotometer Lambda 365 with a 50 mm reflectance sphere (Perkin Elmer, USA).

IR spectra were obtained in the 400–4000 cm^{-1} range using KBr pellet. The Raman spectra were obtained in the range of 200–3600 cm^{-1} . The spectrometer used was a Spectrum GX-FTIR (Perkin Elmer, USA) with 1 cm^{-1} resolution and 15 scans per second.

NMR spectroscopic data were recorded using a Bruker Avance 250 spectrometer (Bruker, USA) operating at 250 MHz for ^1H NMR and 63 MHz for ^{13}C NMR and processed with standard Bruker software. Shifts are given in ppm and coupling constants in Hertz.

Naringenin: ^1H NMR (250 MHz, DMSO) δ 12.15 (s, 1H, C5–OH), 10.79 (s, 1H, C7–OH), 9.59 (s, 1H, C4'–OH), 7.31 (d, J = 8.6 Hz, 2H, C2'), 6.79 (d, J = 8.6 Hz, 2H, C3'), 5.88 (s, 2H, C6 and C8), 5.44 (dd, J = 12.8, 2.8 Hz, 1H, C2), 3.27 (dd, J = 17.2, 12.8 Hz, 1H, C3a), 2.67 (dd, J = 17.2, 2.8 Hz, 1H, C3b). ^{13}C NMR (63 MHz, DMSO) δ = 196.45 (C4), 166.66, 163.50, 162.96 (C5, C7 and C8a), 157.75 (C4'), 128.86 (C1'), 128.38 (CH 2' and 1'), 115.17 (CH 3' and 4'), 101.78 (C4a), 95.80, 94.98 (CG 6 and 8), 78.45 (CH2), 41.98 (CH2–3).

Electron paramagnetic resonance (EPR) spectra were performed on a Bruker EMX Plus spectrometer equipped with a universal high sensitivity cavity (HSW10819 model) using a Bruker nitrogen continuous-flow cryostat. Spectra were acquired under non-saturating conditions. Experimental: microwave frequency, 9.45 GHz; modulation field, 100 kHz; modulation amplitude, 2 G; temperatures are indicated in the caption to the figures. EPR spectra were simulated with the EasySpin toolbox based on MATLAB[®] (Stoll and Schweiger 2006). Simulation of the solution spectrum was performed assuming a Hamiltonian including Zeeman and Hyperfine interactions, $H = \mu_B \mathbf{S} \cdot \mathbf{g} \cdot \mathbf{B} + \mathbf{I} \cdot \mathbf{A} \cdot \mathbf{S}$, where all the symbols have the usual meaning, and \mathbf{g} - and \mathbf{A} -matrices were assumed to be collinear. EPR spectral intensities were evaluated by double integration.

Thermal analysis study

Differential scanning calorimetry was performed with a DSC-Q200 apparatus (TA Instruments, USA) weighing 5–6 mg of sample heated in aluminum pans with lids at a rate of 10 K/min under a nitrogen gas flow of 20 mL/min. Thermal gravimetric analysis (TGA-DTA) was carried out with a Shimadzu DSC-60 instrument (Shimadzu, Japan). Powdered samples weighing 10–11 mg were heated in open aluminum pans at a rate of 10 K/min under a nitrogen gas flow of 40 mL/min.

Single-crystal X-ray diffraction study

The complex obtained in aqueous ethanol solution was dissolved in DMF and recrystallized to obtain a monocrystal. It was analyzed by single crystal X-ray diffractometry.

A 170 K temperature data set was collected on a four circle Oxford Diffraction Gemini CCD S Ultra diffractometer using a graphite monochromated Mo K α source (λ = 0.71073 Å). Measurement yielded 3796 (I) independent reflections of which 2363 were considered observed [$I > 2\sigma(I)$], with an internal consistency R_{int} = 0.0519. Data collection strategy and data reduction followed standard procedures implemented in ChrysAlis Pro software (CrysAlis PRO 2015). Structure determination was achieved routinely by direct methods and difference Fourier. The structure was refined by least squares on F², with anisotropic displacement parameters for non-H atoms. Hydrogen atoms unambiguously defined by the stereochemistry (C–H's and O–H's) were placed at their calculated positions and allowed to ride on their host carbon or oxygen atoms with respect to both their coordinates and their thermal parameters. All calculations to solve and refine the structures and to obtain some derived results were carried out with the computer programs SHELXS97 (Sheldrick 2008), SHELXL2014 (Sheldrick 2015) and Platon (Spek 2009). MERCURY (Macrae et al. 2006) was used to draw molecular views and derive further results. Full use of the CCDC package was also made for searching at the Cambridge Structural Database, Version 5.37 (Groom et al. 2016).

Scavenging activities by the DPPH radical method

The scavenging activities were carried out by the method proposed by Brand-Williams et al. (Brand-Williams et al. 1995). An aliquot of 100 μL of DMF solution containing different naringenin or its copper complex at concentrations up to 20 mN_{NGE} (mili moles of naringenin per liter of solution) was added to 1900 μL of DPPH 65 μM in methanol. The DPPH absorbance of each tube was read at 514 nm after 8 h in the dark at 20 $^{\circ}\text{C}$, when the reaction reaches a semi-steady state. A control solution of DPPH (100 μL de methanol and 1900 μL of DPPH solution) was prepared to estimate the DPPH self-decomposition during the incubation. For each antioxidant concentration, the percentage of DPPH remaining at the semi-steady state was calculated as: % DPPH remaining = $([\text{DPPH}]_{\text{S.S}}/[\text{DPPH}]_{\text{C.S}}) * 100$, where $[\text{DPPH}]_{\text{S.S}}$ is the absorbance of the samples after 8 h and $[\text{DPPH}]_{\text{C.S}}$ is the absorbance of the control DPPH solution. These values were plotted versus the antioxidant concentrations.

DFT computational studies

Crystalline structures were used as initial configuration to make a structure optimization on naringenin and its Cu(II) complex. The structures were confirmed to correspond to a stable ground state by the absence of imaginary frequency in the force constant calculations using tools from density functional theory as implemented in the Gaussian 09 package (Bearing 2009). The method involving the Becke 3-parameter exchange functional together with the Lee–Yang–Parr correlation functional (B3LYP) (Becke 1993; Lee et al. 1988; Miehlich et al. 1989) was used for all the calculations. A Mulliken population analysis (charge and electronic spin density) was conducted with the aim to correlate these data with the compounds' antiradical activities of naringenin, the complex and their relevant radicals using single point. Mulliken population analysis was made in vacuum and considering solvent effect (water and methanol) with polarizable continuum models of solvation (Scalmanian and Frisch 2010).

Results and discussion

Spectroscopic characterization

The UV–Visible spectrum of the ligand in DMF (Fig. 2a) presents two bands. The first one is almost symmetrical, sharp and intense with a maximum at 288 nm (Band II). This band is mainly due to the electronic $\pi \rightarrow \pi^*$ transition that takes place over the A and C rings. The second band (Band I) is also due to a $\pi \rightarrow \pi^*$ transition but on the B ring. This band, located between 315 and 360 nm, is less intense than the first one. Both proposed assignments are in agreement with Shireen et al. who working with TDDFT assigned to pinocembrin (a flavanone like naringenin but with C4'–H, instead C4'–OH) the HOMO-1 \rightarrow LUMO transition at 279 nm located in the π system formed by the A and C rings; and the HOMO \rightarrow LUMO + 1 transition centered at 324 nm, formed by the π system of the B ring (Ajmal Shireen et al. 2017). For the complex in DMF, Band II appears without displacement with respect to naringenin, while Band I presents a slight increase in intensity with respect to the ligand with loss of symmetry towards the visible zone with absorbance beyond 360 nm. The spectral modification could be assigned to charge transfer either ligand–metal or metal–ligand, transitions mainly produced on the C4–O–Cu and C5–O–Cu bonds. For the complex in DMF, but at 7 mM (3900 ppm), a $d-d$ electron transition band with low intensity is observed centered at 650 nm, while for naringenin in similar conditions no absorbance over 400 nm is present (Fig. 2c).

In water at neutral pH, the spectrum of naringenin is the same as in DMF. For the complex, the absorptivity of Band II appears diminished and its λ_{max} is displaced to 290 nm, and the intensity of band I appears increased.

In solid state (Fig. 2d), band II is located at 260–300 nm for both compounds, and band I appears strongly displaced to the visible (from 320–380 nm to 380–490 nm). The complex presents also a band in the visible region centered at 650 nm due to the $d-d$ transitions of the Cu(II) (Lever 1984).

The complex was characterized by FT-IR and Raman spectroscopy. Figures 3 (IR) and 4 (Raman) present the vibrational spectra of naringenin and of the copper (II) naringenin complex.

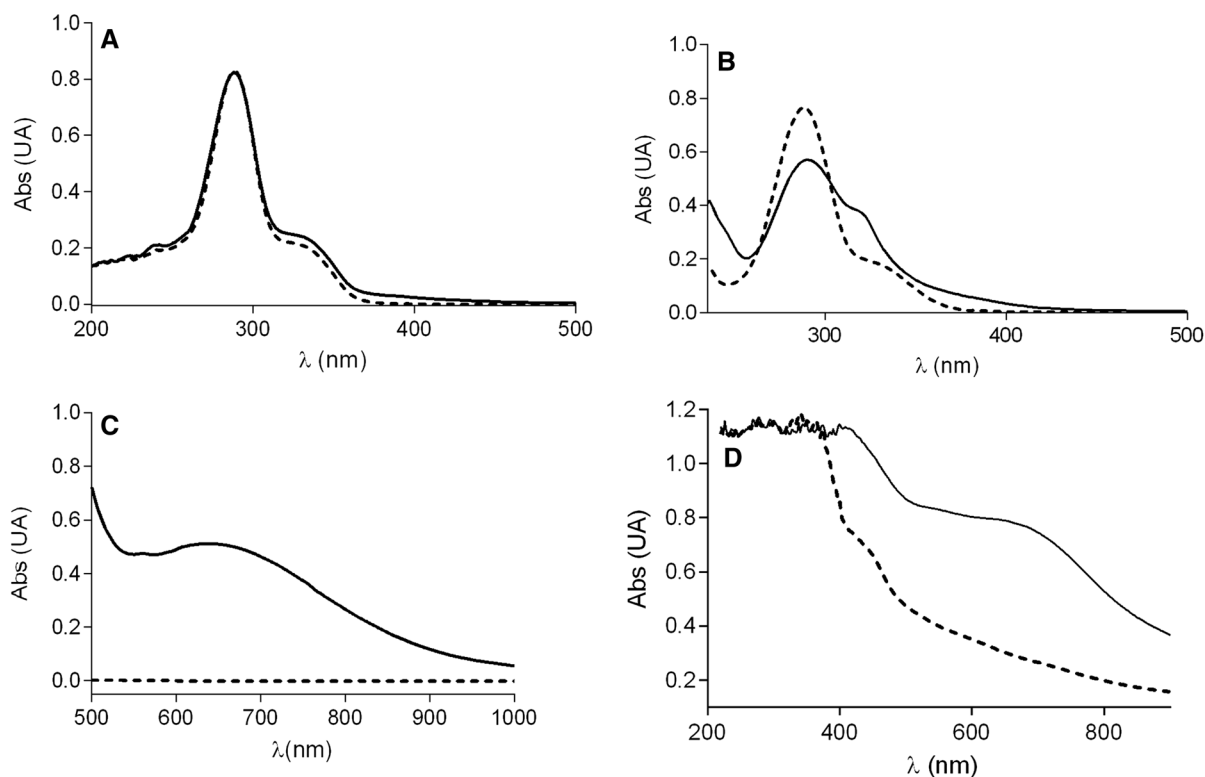


Fig. 2 UV/Vis spectra of the copper (II) naringenin complex (full line), and naringenin (dashed line). **a** in DMF: naringenin 0.05 mM and copper (II) naringenin complex 0.025 mM; **b** in water at neutral pH: naringenin 0.05 mM and copper (II)

naringenin complex 0.025 mM; **c** in DMF: naringenin 15 mM and copper (II) naringenin complex 8 mM; **d** in solid state by diffuse reflectance spectroscopy

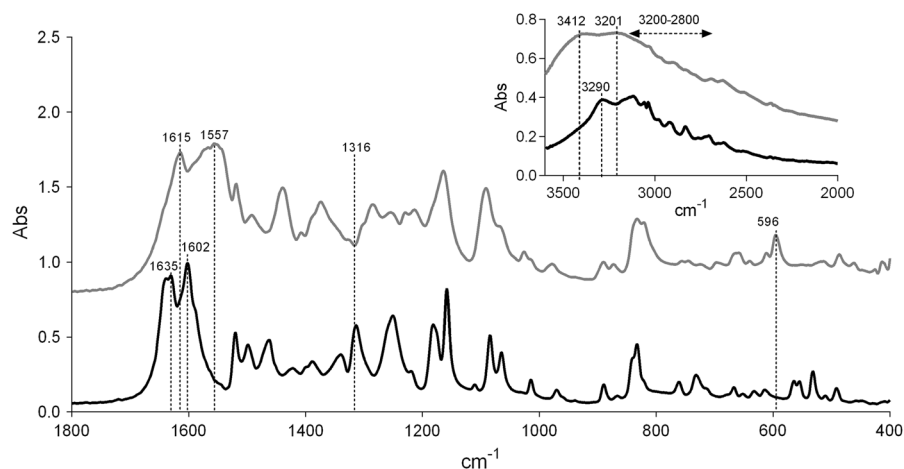
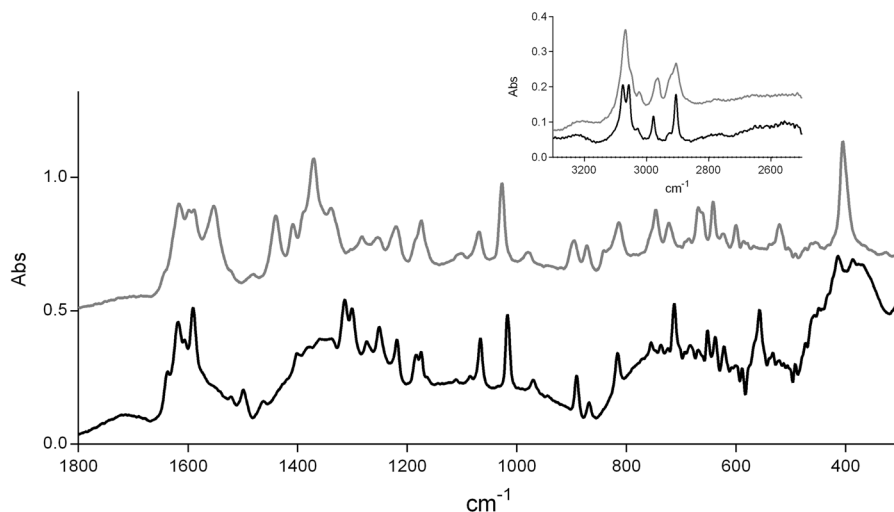


Fig. 3 IR spectra for naringenin (black—bottom line) and for the copper (II) naringenin complex (gray—upper line)

The band assignments were made according to Unsalan et al. (Unsalan et al. 2009), who studied experimentally and theoretically the molecular structures of naringenin. The most intense absorption for

the phenolic groups stretching appears at 3290 cm^{-1} for naringenin and at 3201 cm^{-1} for the complex. The complex shows an additional band at 3412 cm^{-1} , which would correspond to the O–H stretching

Fig. 4 Raman spectra for naringenin (black—bottom line) and for the copper (II) naringenin complex (gray—upper line)



assigned to coordinated water (Uivarosi et al. 2016). The IR absorption between 3200 and 2800 cm^{-1} correspond, for both molecules, to C–H stretches. By Raman resonance, these bands were more defined.

The most intense absorption, due to the C=O stretching, occurred in the region of 1635 cm^{-1} (IR) for naringenin, whereas for the complex it appeared at 1615 cm^{-1} (IR). The displacement to lower frequencies indicates weakening of the double bond by coordination to the copper ion. Tan et al. synthesized and characterized naringenin, hesperetin and apigenin copper (II) complexes. They presented similar IR assignments and reported the same displacement of the carbonyl signal at lower frequencies when the flavonoids were coordinated to copper (Tan et al. 2009). Centered at 1602 (IR) (1618 – 1555 cm^{-1} in Raman) for naringenin, and at 1557 cm^{-1} (IR) (1591 – 1555 cm^{-1} in Raman) for the complex, stretching bands corresponding to C=C are observed.

A particular band centered at 1316 cm^{-1} (IR and Raman) for naringenin, is not present in the complex. We suggest that it can be assigned to a C5–OH deformation and it could be a main vibrational evidence of the complex formation at the C4–O and C5–O position. This assumption is in accordance with Unsalan et al. who studied by DFT the FT-IR of naringenin and assigned this absorption at 1314 cm^{-1} to $\delta\text{C–OH} + \nu_{\text{CO}}$ (Unsalan et al. 2009).

Further evidence for complex formation was a low-intensity band at 596 cm^{-1} (IR), present in the complex but not in the naringenin spectrum. This band was attributed to a M–O stretching. This

assignment is supported by Nakamoto, who studying the FT-IR of complexes of β -diketones and Cu(II), assigned the IR region close to 610 cm^{-1} to $\delta_{\text{M–ring}} + \nu_{\text{M–O}}$ (Nakamoto 2009).

The ^1H NMR spectra obtained for naringenin and for the complex are shown in Fig. 5. The naringenin ^{13}C NMR spectra are in agreement with other previously reported (Agrawal and Schneider 1983). The naringenin ^1H NMR spectra was identical to other previously reported (Pouchert and Behnke 1993). For the complex, it was obtained a drastically different spectral profile with wide signals due to the presence of the paramagnetic copper atom. The signals appear enlarged; this fact prevents integration and determination of the multiplicities of the hydrogen atoms. Despite of this, we could see the absence of the proton located on the 5-OH hydroxyl group (δ 12.15 in naringenin), indicating that it is in the form of alkoxide. In addition, we suggest that the band centered at δ 9.6 corresponds to the hydroxyl group 4'-OH (which does not undergo displacement with respect to naringenin), and to the signal of the 7-OH that was displaced due to the presence of the alkoxide formed in the same ring. These results are compatible with chelation and charge neutralization by the copper (II) metal center in the 5-alkoxi 4-keto position. In addition, no ethanol signals (typical at 1.1 and around 4), or acetate ion (near to 2 ppm) are observed, so they are not part of the complex.

Wang et al. (2006) synthesized a complex with Zn(II) and naringenin. They report a similar

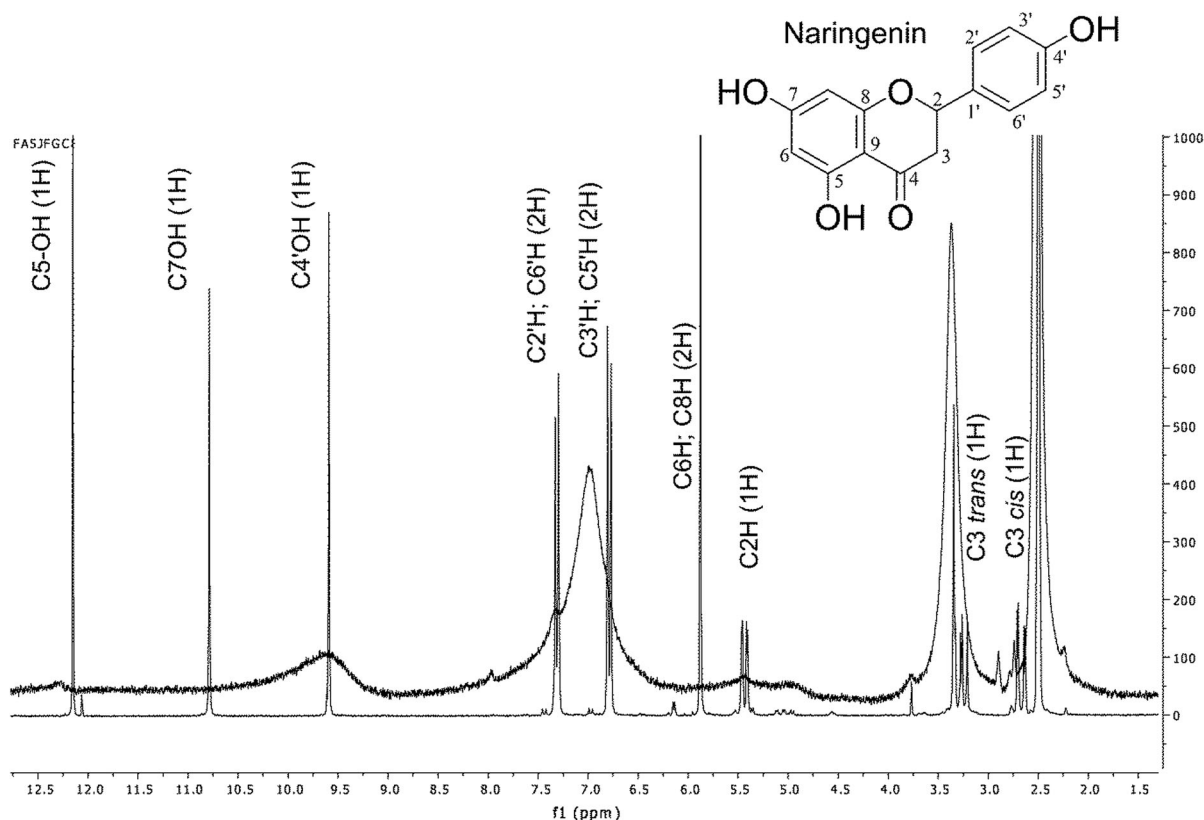


Fig. 5 ^1H NMR spectrum for naringenin (defined signal) and its Cu(II) complex (broad signal). The 2D structure of naringenin is shown as inset

assignment that us with broadening of the signals and loss of the C5–OH signal in the complex (Wang et al. 2006).

X-band EPR spectra of a frozen solution in DMSO and a polycrystalline sample of the copper (II) naringenin complex are shown in Fig. 6.

The EPR spectrum of the frozen DMSO solution of the Cu^{2+} complex ($S = 1/2$) (spectrum a) shows nearly axial symmetry with well solved hyperfine structure with the Cu nucleus ($I = 3/2$) at $g_{//}$. Simulation of this spectrum (dashed line) yielded $g_{1,2,3} = 2.290, 2.060, 2.053$ and $A_{1,2,3} = 15.8, 2.4, \text{n.d. mT}$ (n.d., non-detectable). These values, which are within the typical ones reported for Cu (II) complexes in nearly square planar coordination with O-ligands, indicate a dx^2-y^2 magnetic ground state for the Cu(II) ions. In line with the solution complex, the EPR spectrum of the polycrystalline sample at room temperature (spectrum b in Fig. 6) shows also axial symmetry with detectable hyperfine structure at $g_{//}$ but broadened due to inter-copper dipole–dipole interactions.

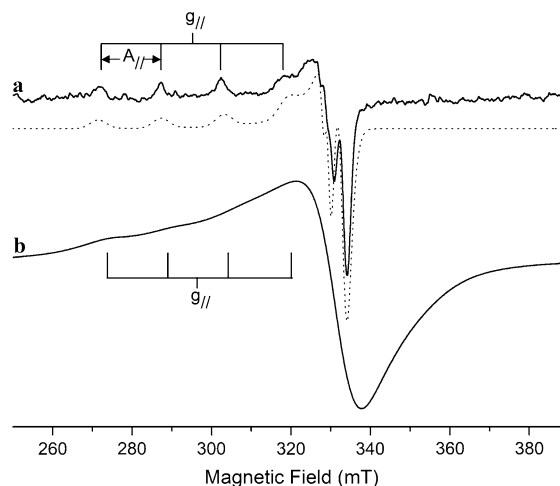


Fig. 6 X-band EPR spectra of the copper (II) naringenin complex: a- in DMSO frozen solution (140 K) and b- solid state at room temperature; dashed line: theoretical simulation

No significant differences were observed in the EPR spectra of the solid taken in the range of 120 K–room temperature (Fig. 7), apart from the typical

dependence of the EPR signal intensity with temperature, the larger the temperature, the lower the intensity. The fact that the hyperfine structure is partially solved in these spectra indicates that the Cu(II) ions are very weakly coupled by exchange. This is in line with the crystal lattice of Cu(II) ions observed in Fig. 10, which is an 1-D arrangement linked by non-covalent interactions, that form a weakly exchange coupled systems (Neuman et al. 2012; Rizzi et al. 2016). This conclusion is also reinforced by the temperature variation of the intensity (I) of the solid state EPR spectra (Fig. 7).

Note that the intensity of $S = 1/2$ EPR spectra under non-saturating conditions are proportional the magnetic susceptibility χ . These data, analyzed assuming a Curie–Weiss behavior ($I = \text{constant}/(T - \Theta)$), where the constant is proportional to the Curie constant C , and Θ is the Weiss temperature, a parameter proportional to the magnitude to the exchange interaction between copper ions, yielded a null Θ -value within the experimental error. The fact that the positions of the g_{\parallel} - and A_{\parallel} -features in both solid and solution complexes are rather similar (Fig. 6) constitutes a strong evidence that the structure of the complex in solid state determined by X-ray crystallography (presented below) is kept upon dissolution in DMSO solvent.

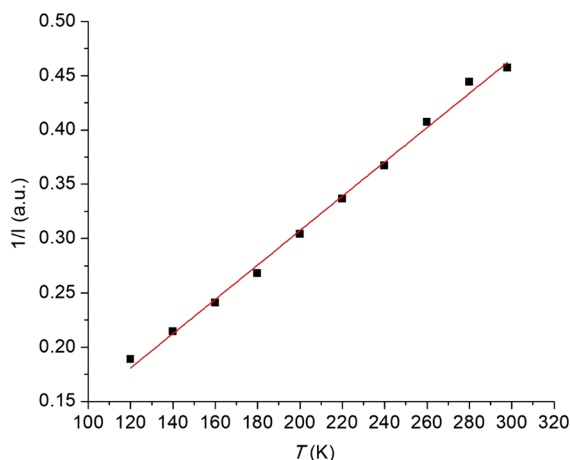


Fig. 7 Plot of $1/I$ versus T , where I is the intensity of the EPR spectra evaluated by double integration. A least square linear fit with a Curie–Weiss model to the data yielded slope = 0.00158 (3), intercept = $-0.08(8)$, square $R = 0.995$, where the slope and the intercept are proportional to C^{-1} (C = Curie constant) and Θ , respectively (see main text for more details)

The EPR spectrum of the solid shows also a broad weak resonance line at ~ 160 mT (see inset Supplementary material, Figure EPR). This transition, which must not be observed in an isolated mononuclear copper (II) compound, has been detected in a few cases in 1D—systems containing Cu(II) ions coupled by dipole–dipole interactions, as could be the case of Cu^{2+} complex with naringenin according to Fig. 8 (Bencini and Gatteschi 1990). The analysis of this phenomenon is beyond of the aims of this paper.

Thermal study

The thermal behavior of the complex was determined by TGA and DSC. First, the DSC thermogram for naringenin (Fig. 8) presents 3 peaks: the first one at 202°C is related to the glass transition; the second endothermic peak at 250°C without loss of mass is related to the melting point of naringenin, which is consistent with the value reported in the literature (CRC Handbook of Chemistry and Physics 93th edition); the third endothermic event (centered at 283°C) was attributed to thermal decomposition of naringenin, which was previously reported for similar flavanones (Ferreira et al. 2017). For the complex, an endothermic peak at 161°C can be ascribed to the loss of 2 coordinated water molecules, which agree with a weight loss of 5.1% by TGA. The thermal event at 202°C is related to the melting point of the complex, showing a decrease of the reticular energy comparing with naringenin. The last endothermic event with

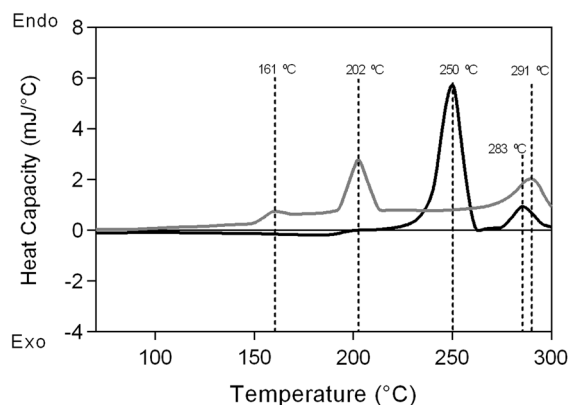


Fig. 8 DSC of naringenin (black line) and copper (II) naringenin complex (grey line). under nitrogen atmosphere, heating rate $10^\circ\text{C min}^{-1}$. Sample mass 5.83 mg of complex and 5.05 mg of naringenin

matter loss centered at 291 °C is related to thermal decomposition of the ligand.

Single-crystal X-ray diffraction study

The crystals obtained by recrystallization in DMF were analyzed by single crystal X-ray. These crystals are triclinic, space group P-1, with $a = 7.3581(7)$ Å, $b = 9.6904(7)$ Å, $c = 12.2937(8)$ Å, $\alpha = 86.098(6)^\circ$, $\beta = 73.088(7)^\circ$, $\gamma = 85.224(7)^\circ$, $V = 834.87(12)$ Å³ and $Z = 4$. Crystallographic results are given in Table 1. The molecular structure of the complex, [Cu(C₁₅H₇O₅)₂(C₃H₇O₁N₁)₂], is monomeric with a

Cu(II) hexacoordinated center (Fig. 9). The coordination sphere is formed by two oxygen atoms from two bidentate naringenin ligands and one oxygen atom from two dimethylformamide molecules, with metal–O distances in the range 1.900(2)–2.560(5) Å (Table 2). According to this result the nomenclature of the complex is *trans*-di(*N,N*-dimethylmethanamide)bis(7-hydroxy-2-(4-hydroxyphenyl)-4-oxo-5-chromanolato) copper (II).

The crystal structure is supported by H-bonds between the uncoordinated naringenin OH and the oxygen atom of the DMF (O(7)–H(7)–O(6)), showing columns along an axis (Table 3, Fig. 10a). In spite of

Table 1 Crystal and structure refinement data

Crystal data	
C ₃₆ H ₃₆ CuN ₂ O ₁₂	$Z = 1$
$M_r = 752.22$	$F(000) = 391$
Triclinic, $\bar{P}1$	$D_x = 1.496$ Mg m ⁻³
Hall symbol: -P 1	Mo $K\alpha$ radiation, $\lambda = 0.71073$ Å
$a = 7.3581(7)$ Å	Cell parameters from 1162 reflections
$b = 9.6904(7)$ Å	$\theta = 4.3$ – 26.2°
$c = 12.2937(8)$ Å	$\mu = 0.72$ mm ⁻¹
$\alpha = 86.098(6)^\circ$	$T = 173$ K
$\beta = 73.088(7)^\circ$	Prism, red
$\gamma = 85.224(7)^\circ$	$0.3 \times 0.3 \times 0.2$ mm ³
$V = 834.87(12)$ Å ³	
Data collection	
Oxford diffraction Gemini CCD S ultra diffractometer	3796 Independent reflections
Radiation source: fine-focus sealed tube	2363 Reflections with $I > 2\sigma(I)$
Graphite monochromator	$R_{\text{int}} = 0.052$
ω scans, thick slices	$\theta_{\text{max}} = 29.1^\circ$, $\theta_{\text{min}} = 3.7^\circ$
Absorption correction: multi-scan <i>CrysAlis PRO</i> , Oxford Diffraction (2009)	$h = -5 \rightarrow 9$
$T_{\text{min}} = 0.928$, $T_{\text{max}} = 1.000$	$k = -12 \rightarrow 12$
6620 measured reflections	$l = -15 \rightarrow 15$
Refinement	
Refinement on F^2	Zero restraints
Least-squares matrix: full	Hydrogen site location: mixed
$R[F^2 > 2\sigma(F^2)] = 0.071$	H atoms treated by a mixture of independent and constrained refinement
$wR(F^2) = 0.153$	$w = 1/[\sigma^2(F_o^2) + (0.0441P)^2 + 0.2509P]$ where
$S = 1.06$	$P = (F_o^2 + 2F_c^2)/3$
3796 Reflections	$(\Delta/\sigma)_{\text{max}} < 0.001$
246 Parameters	$\Delta_{\text{max}} = 0.63$ e Å ⁻³
	$\Delta_{\text{min}} = -0.57$ e Å ⁻³

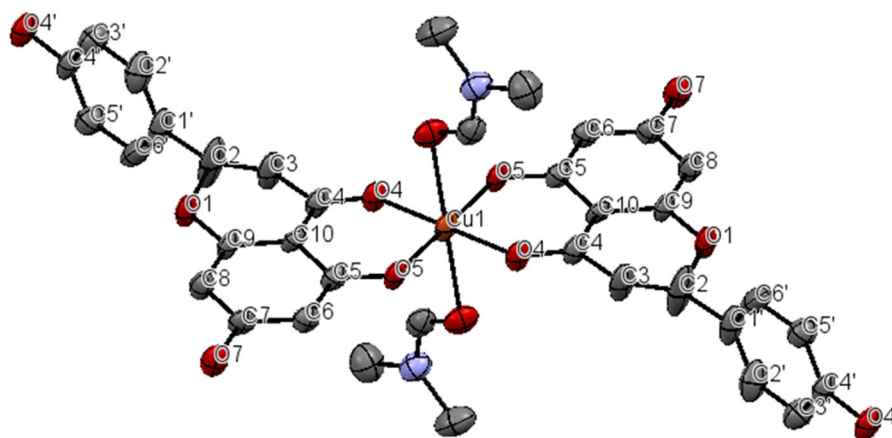


Fig. 9 Thermal ellipsoids of *trans*-di(*N,N*-dimethylmethanamide)bis(7-Hydroxy-2-(4-hydroxyphenyl)-4-oxo-5-chromanolato) copper (II) drawn at the 50% probability level. H atoms were removed for clarification

Table 2 Selected bond distances (Å)

Interaction	Cu(II)–naringenin	Naringenin ^a
Cu–O4	1.933(5)	–
Cu–O5	1.900(2)	–
Cu–O6	2.560(3)	–
C4–O4 (C=O)	1.260(5)	1.265(5)
C5–O5 (C–OH)	1.303(5)	1.353(5)

^aPreviously reported, CSD refcode: DOLRIF

the presence of aromatic rings there are no π – π interactions in the structure, while the packing is assisted by weak C–H···O interactions (Table 3) between naringenin's phenyl group and one of the DMF's methyl group (Fig. 10b); and by CH– π interactions in c direction (Fig. 10c). The overall effect of these weak interactions, uniformly distributed in space, is the formation of a three-dimensional structure where each molecule is linked to ten different neighbors. Other interesting result is that the bond lengths in the crystal of C₄=O₄ and C₅–OH₅ groups are shorter in the complex with respect to the

flavonoid alone. It is because in the complex these groups are interacting with the copper but not are participating in intermolecular attractions, what yes occurs in the naringenin crystalline structure (Table 4).

It is well known that the acid strength of the ionizable hydrogens of naringenin follows the order: 7-OH > 4'-OH > 5-OH (Agrawal and Schneider 1983). However, in the crystal structure the only ionized hydrogen is the corresponding to C₅–OH. This is because copper induces the loss of the proton located at the C₅-hydroxy C₄-keto position, which is the unique position where naringenin can act as a bidentate chelate.

Scavenging activities of naringenin and its copper (II) complex

Flavanones are not among the flavonoids that have higher antioxidant capability (Rice-Evans et al. 1996). This is because the phenolic rings A and B are not conjugated, since C₂ and C₃ have sp³ hybridization. Therefore, ring B is almost perpendicular to rings A and C. Figure 11 shows that naringenin had higher

Table 3 Selected interactions distances (Å)

	Donor–H	Acceptor	D–H	H···A	D···A	D–H···A
^a 1 – x, – y, – z	O(7)–H(7)	O(6) ^a	0.77(5)	1.98(5)	2.729(5)	167(5)
^b – 1 + x, y, 1 + z	O(4')–H(4')	O(5) ^b	0.91(7)	1.81(7)	2.708(4)	169(7)
^c – 1 + x, – 1 + y, 1 + z	C(16)–H(16A)	O(4') ^c	0.98	2.86(2)	3.189(6)	92(6)
^d – x, – y, 1 – z	C(17)–H(17C)	Cg(1) ^d	0.98	2.90(3)	3.573(6)	127(5)
	C(3')–H(3')	Cg(2) ^d	0.98	2.86(3)	3.618(5)	137(6)

Fig. 10 View of three-dimensional structure **a** Packing view projected down a showing H-bond between O(7)–H(7) and O(6)¹, **b** C(16)–H(16)–O(4')² weak interaction **c** C(17)–H(17C)– π (Cg1)³ and C(3')–H(3')– π (Cg2)³ along c axis. ¹1 – x, – y, – z, ²– 1 + x, – 1 + y, 1 + z, ³– x, – y, 1 – z

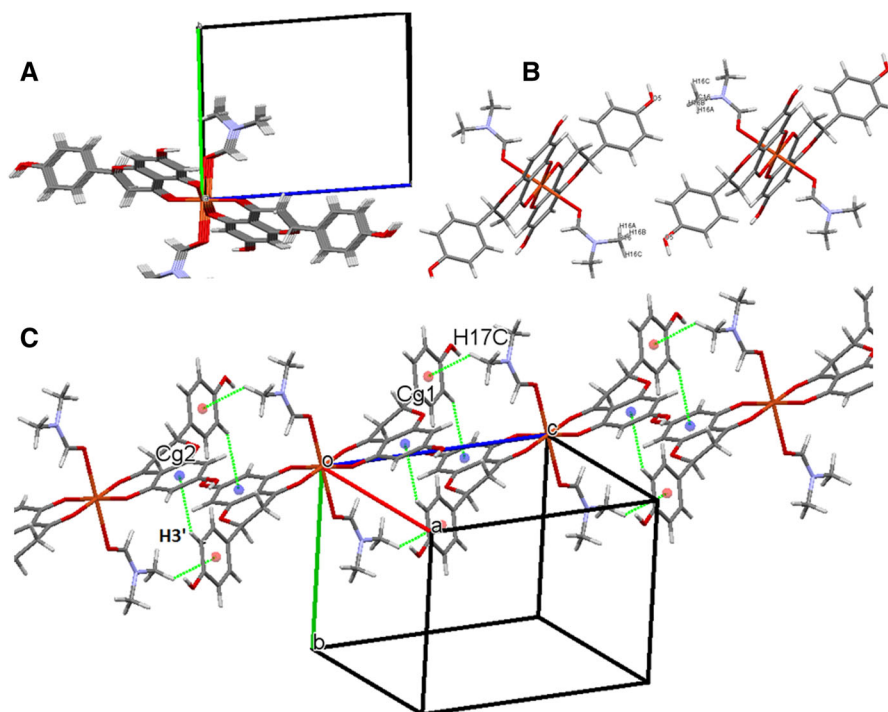


Table 4 Selected interactions distances in both compounds (Å)

Atoms	Cu(II)Naringenin	Naringenin ^a
C4–O4	1.260(5)	1.265(5)
(C=O)		
C5–O5	1.303(5)	1.353(5)
(C–OH)		

^aPreviously reported, CSD refcode: DOLRIF

antiradical activity when is chelating Cu(II) than when it is free. De Sousa et al. has previously screened the antiradical activity of quercetin, rutin and 3-hydroxyflavone and some parent complexes of Cu(II) and Fe(II) by using DPPH. They found that the complexed flavonoids were more effective radical scavengers than the free flavonoids (de Souza and De Giovanni 2004). Pekal et al. also reported that the quercetin copper (II) complex is much more effective as free radical scavenger than the flavonoid alone (Pekal et al. 2011). They did not make additional experiments to understand the reason.

Due to the lack of resonance between the B ring and the rest of the molecule, complex formation should not

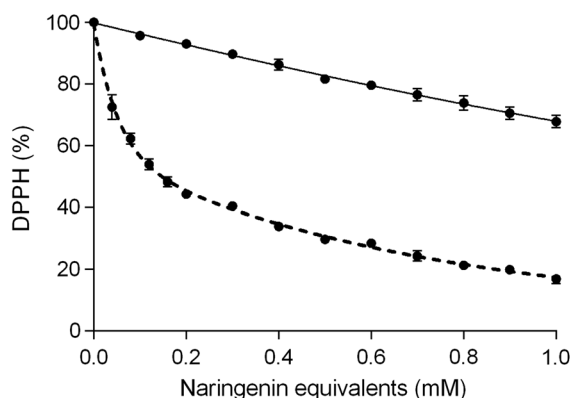


Fig. 11 Remaining DPPH (%) at the end of the reaction as a function of the concentration of naringenin free (full line) or chelating Cu(II) (dashed line). Mean and SD of two independent values are presented

affect the reactivity of the C4'–OH group, which is the main reactive group of naringenin against radicals (Jabbari et al. 2014) and therefore, naringenin free or complexed must have the same antiradical activity.

The second phenolic group that can react with DPPH is the C7–OH. According to the Mulliken population analysis (Table 5), in the complex the C5–O[–] charge is delocalized reducing the net charge of copper and increasing the negative charge on C4–O

Table 5 Charge and electronic spin density (in parentheses) from Mulliken population analysis in vacuum (white), methanol (bold) and water (italics) for naringenin, naringenin Cu(II) complex and some of their relevant phenolic radicals

	Relevant atoms				
	C5–O	C4–O	C4'–O	C7–O	Cu
Naringenin	– 0.347	– 0.389	– 0.358	– 0.345	–
	–	–	–	–	–
	– 0.366	– 0.419	– 0.385	– 0.366	–
	–	–	–	–	–
	<i>– 0.367</i>	<i>– 0.42</i>	<i>– 0.386</i>	<i>– 0.367</i>	–
Naringenin C7–O* (without 7-H*)	–	–	–	–	–
	– 0.338	– 0.363	– 0.356	– 0.307	–
	(– 0.016)	(0.081)	–	(0.648)	–
	– 0.357	– 0.385	– 0.385	– 0.364	–
	(– 0.018)	(0.084)	–	(0.606)	–
Naringenin C5–O* (without 5-H*)	– 0.358	– 0.385	– 0.385	– 0.366	–
	<i>(– 0.018)</i>	<i>(0.085)</i>	–	<i>(0.604)</i>	–
	– 0.264	– 0.271	– 0.357	– 0.346	–
	(0.617)	(0.091)	–	(– 0.012)	–
	– 0.343	– 0.339	– 0.385	– 0.362	–
Complex (without 5-H ⁺)	(0.536)	(0.044)	–	(– 0.017)	–
	– 0.346	– 0.341	– 0.385	– 0.363	–
	<i>(0.534)</i>	<i>(0.043)</i>	–	<i>(– 0.017)</i>	–
	– 0.650	– 0.528	– 0.359	– 0.351	1.342
	(0.017)	(0.021)	–	(0.000)	(0.840)
Complex C7–O* (without 5-H ⁺ , neither 7-H*)	– 0.645	– 0.532	– 0.385	– 0.370	1.254
	(0.070)	(0.062)	–	(0.000)	(0.711)
	– 0.645	– 0.532	– 0.386	– 0.370	1.253
	<i>(0.070)</i>	<i>(0.062)</i>	–	<i>(0.000)</i>	<i>(0.711)</i>
	– 0.621	– 0.495	– 0.357	– 0.313	1.261
Complex C7–O* (without 5-H ⁺ , neither 7-H*)	(0.073)	(0.115)	–	(0.650)	(0.711)
	– 0.634	– 0.506	– 0.385	– 0.368	1.257
	(0.065)	(0.121)	–	(0.611)	(0.712)
	– 0.635	– 0.506	– 0.386	– 0.369	1.257
	<i>(0.064)</i>	<i>(0.121)</i>	–	<i>(0.609)</i>	<i>(0.712)</i>

and C7–O, what favors the homolytic cleavage of the C7O–H bond. For another hand, the charge density of Cu in the complex is 1342 (in vacuum). When the homolytic rupture occurs and C7–O* radical is formed, the charge density on copper decreases further (to 1.253 in vacuum). This indicates that part of the unpaired electron charge is being transferred to copper. So, it acts as an electronic density acceptor. These two effects justify theoretically the experimental fact that naringenin has greater antiradical activity when it is forming the copper complex. In simulated media with solvents (water and ethanol), this behavior

is also evident, but with slight differences in the charge and spin densities.

In addition to the reported in this paper, it must be taken into account that when Cu(II) is present it could exist coupled reaction that stabilize either, reaction intermediates or products. Furthermore, the antiradical enhancement could even be associated to reactions where the Cu(II)–Cu(I)–Cu(II) cycle is present (Arif et al. 2017).

Chelation of metals with flavonoids reduces the redox potential of both. This, in turn, retard the metal propensity to promote free radical formation (Selvaraj et al. 2014a), and enhance the interaction of the

flavonoid with biological membranes (Selvaraj et al. 2014b). Moreover, the antioxidant enhancement of naringenin and hesperetin when they are forming Cu(II) complexes with 1,10-phenanthroline as co-ligand would seem to be the reason of the improvement of the apoptotic action against malignant A549 cells by a mitochondria-independent pathway (Tamayo et al. 2016).

It has been demonstrated that naringenin ameliorates Alzheimer's disease type neurodegeneration with cognitive impairment in rat models (Khan et al. 2012). This disease is oxidative stress mediated. So, it is interesting to suspect that the delivery of naringenin in the form of Cu(II) complex, with better antiradical activity, could help to increase its cytotoxicity against malignant cells and more efficacies in the treatment of neurodegenerative diseases oxidative stress mediated.

Conclusions

The complex *trans*-di(aqua) bis(7-hydroxy-2-(4-hydroxyphenyl)-4-oxo-5-chromanolato) copper (II) was obtained from *Citrus* processing waste economically and easily through a green process with a simple downstream. The compound was characterized by spectroscopic techniques (UV/Vis, IR, Raman, NMR and EPR), and by thermal analysis (TG and DSC). Its analogous DMF complex was obtained by crystallization of the aqua complex in DMF, and its structure was obtained by single-crystal X-ray diffraction. The results allow concluding that copper (II) binds to naringenin through the C4-keto C5-hydroxy position. The crystalline structure shows that 2 naringeninate ions in the same plane are chelated to copper (II) in *trans* configuration while 2 molecules of secondary ligands (water or DMF) are up and down this plane. EPR demonstrates that the structure in solid state determined by X-ray persist upon dissolution. IR, UV-Vis, and EPR spectroscopic data analysis gave new clues to understand the complex formation that might surely be used to characterize similar metal complexes.

It was reported that naringenin ameliorates Alzheimer's disease type neurodegenerative with cognitive impairment in rat models, being this disease oxidative stress mediated. Coordination to copper (II) enhances the antiradical activity of naringenin strongly, since

copper acts as an electronic density acceptor stabilizing the produced radical. So, it is interesting to suspect that the delivery of naringenin in the form of Cu(II) complex could help to increase the efficacy of this ligand in the treatment of this and other similar neurodegenerative diseases. The next step is to assay properties and toxicity of the complex to test its scope.

Acknowledgements We thank Universidad Nacional de Salta (Proyecto CIUNSa No 2227), Agencia Nacional de Promoción Científica y Tecnológica de Argentina (PICT 2012 No 0696) and Secretaría de Políticas Universitarias (PNo. 33-63-029-2014) for financial support. The authors acknowledge ANPCyT (Project No. PME 2006-01113) for the purchase of the Oxford Gemini CCD diffractometer. We also acknowledge Departamento de Física de la Materia Condensada, CNEA for the use of TGA facilities and Dra. Gabriela Levy for her helpful assistance. Universidad Nacional de Catamarca (UNCa) is also appreciated for their computation supports. G. Céliz, S. Suarez, C. D. Brondino, and F. Doctorovich are members of the Research Career of CONICET.

References

- Agrawal PK, Schneider H-J (1983) Deprotonation induced ¹³C NMR shifts in phenols and flavonoids. *Tetrahedron Lett* 24:177–180. [https://doi.org/10.1016/S0040-4039\(00\)81359-3](https://doi.org/10.1016/S0040-4039(00)81359-3)
- Ajmal Shireen P, Abdul Mujeeb VM, Muraleedharan K (2017) Theoretical insights on flavanones as antioxidants and UV filters: a TDDFT and NLMO study. *J Photochem Photobiol B* 170:286–294. <https://doi.org/10.1016/j.jphotobiol.2017.04.021>
- Amic D, Davidovic-Amic D, Beslo D, Rastija V, Lucic B, Trinajstić N (2007) SAR and QSAR of the antioxidant activity of flavonoids. *Curr Med Chem* 14:827–845
- Arif H, Sohail A, Farhan M, Rehman AA, Ahmad A, Hadi SM (2017) Flavonoids-induced redox cycling of copper ions leads to generation of reactive oxygen species: a potential role in cancer chemoprevention. *Int J Biol Macromol*. <https://doi.org/10.1016/j.ijbiomac.2017.08.049>
- Barreca D et al (2017) Flavanones: citrus phytochemical with health-promoting properties. *BioFactors* 43:495–506. <https://doi.org/10.1002/biof.1363>
- Bearpark M et al (2009) Gaussian 09, Revision A. 01. Gaussian Inc, Wallingford CT
- Becke AD (1993) Becke's three parameter hybrid method using the LYP correlation functional. *J Chem Phys* 98:5648–5652
- Bencini A, Gatteschi D (1990) Spectra in extended lattices. Electron paramagnetic resonance of exchange coupled systems. Springer, Berlin. <https://doi.org/10.1007/978-3-642-74599-7>
- Brand-Williams W, Cuvelier ME, Berset C (1995) Use of a free radical method to evaluate antioxidant activity. *LWT Food Sci Technol* 28:25–30

- Brodowska K (2013) Naringenin complexes with copper ions: potentiometric studies. *Biotechnol Food Sci* 77:44–53
- Cavia-Saiz M, Busto MD, Pilar-Izquierdo MC, Ortega N, Perez-Mateos M, Muñiz P (2010) Antioxidant properties, radical scavenging activity and biomolecule protection capacity of flavonoid naringenin and its glycoside naringin: a comparative study. *J Sci Food Agric* 90:1238–1244. <https://doi.org/10.1002/jsfa.3959>
- CrysAlis PRO (2015) Rigaku oxford diffraction. Rigaku Corporation, Tokyo
- de Souza RFV, De Giovani WF (2004) Antioxidant properties of complexes of flavonoids with metal ions. *Redox Rep* 9:97–104. <https://doi.org/10.1179/135100004225003897>
- Erlund I (2004) Review of the flavonoids quercetin, hesperetin, and naringenin. Dietary sources, bioactivities, bioavailability, and epidemiology. *Nutr Res* 24:851–874
- Ferreira LMB, Kobelnik M, Regasini LO, Dutra LA, da Silva Bolzani V, Ribeiro CA (2017) Synthesis and evaluation of the thermal behavior of flavonoids. *J Therm Anal Calorim* 127:1605–1610. <https://doi.org/10.1007/s10973-016-5896-6>
- Groom CR, Bruno IJ, Lightfoot MP, Ward SC (2016) The Cambridge structural database. *Acta Crystallogr Sect B* 72:171–179. <https://doi.org/10.1107/S2052520616003954>
- Ilkay EO, Seyed FN, Maria D, Gian CT, Kowsar M, Seyed MN (2015) Naringenin and atherosclerosis: a review of literature. *Curr Pharm Biotechnol* 16:245–251. <https://doi.org/10.2174/1389201015666141202110216>
- Jabbari M, Mir H, Kanaani A, Ajloo D (2014) Kinetic solvent effects on the reaction between flavonoid naringenin and 2,2-diphenyl-1-picrylhydrazyl radical in different aqueous solutions of ethanol: an experimental and theoretical study. *J Mol Liq* 196:381–391. <https://doi.org/10.1016/j.molliq.2014.04.015>
- Khan MB et al (2012) Naringenin ameliorates Alzheimer's disease (AD)-type neurodegeneration with cognitive impairment (AD-TNDCI) caused by the intracerebroventricular-streptozotocin in rat model. *Neurochem Int* 61:1081–1093. <https://doi.org/10.1016/j.neuint.2012.07.025>
- Klein JA, Ackerman SL (2003) Oxidative stress, cell cycle, and neurodegeneration. *J Clin Invest* 111:785–793. <https://doi.org/10.1172/JCI200318182>
- Lee C, Yang W, Parr RG (1988) Development of the Colle-Salvetti correlation-energy formula into a functional of the electron density. *Phys Rev B* 37:785
- Lever A (1984) Electronic spectra of dn ions. *Inorgan Electr Spectr* 2:376–611
- Macrae CF et al (2006) Mercury: visualization and analysis of crystal structures. *J Appl Crystallogr* 39:453–457. <https://doi.org/10.1107/S002188980600731X>
- Miehlich B, Savin A, Stoll H, Preuss H (1989) Results obtained with the correlation energy density functionals of Becke and Lee, Yang and Parr. *Chem Phys Lett* 157:200–206
- Nakamoto K (2009) Infrared and Raman spectra of inorganic and coordination compounds, applications in coordination, organometallic, and bioinorganic chemistry. Wiley Inc., New York, pp 96–98
- Neuman NI, Franco VG, Ferroni FM, Baggio R, Passeggi MCG, Rizzi AC, Brondino CD (2012) Single crystal EPR of the mixed-ligand complex of copper (II) with L-glutamic acid and 1,10-phenanthroline: a study on the narrowing of the hyperfine structure by exchange. *J Phys Chem A* 116:12314–12320. <https://doi.org/10.1021/jp308745e>
- Patel K, Singh GK, Patel DK (2014) A review on pharmacological and analytical aspects of naringenin. *Chin J Integr Med*. <https://doi.org/10.1007/s11655-014-1960-x>
- Pekal A, Biesaga M, Pyrzynska K (2011) Interaction of quercetin with copper ions: complexation, oxidation and reactivity towards radicals. *Biomaterials* 24:41–49. <https://doi.org/10.1007/s10534-010-9372-7>
- Poore HD (1934) Recovery of naringin and pectin from grapefruit residue. *Ind Eng Chem* 26:637–639. <https://doi.org/10.1021/ie50294a011>
- Pouchert C, Behnke J (1993) Aldrich® Library of ¹³C and ¹H FT-NMR Spectra. Aldrich Chemical Co, St. Louis
- Pulley GN (1936) Solubility of Naringin in water. *Ind Eng Chem* 8:360. <https://doi.org/10.1021/ac50103a020>
- Rice-Evans CA, Miller NJ, Paganga G (1996) Structure-antioxidant activity relationships of flavonoids and phenolic acids. *Free Radic Biol Med* 20:933–956
- Rizzi AC, Neuman NI, González PJ, Brondino CD (2016) EPR as a tool for study of isolated and coupled paramagnetic centers in coordination compounds and macromolecules of biological interest. *Eur J Inorg Chem*. <https://doi.org/10.1002/ejic.201690002>
- Robin J, Blanco S, Macoritto A, Soria F, Geronazzo H (2007) Obtención de prunina, ramnosa y naringenina por hidrólisis ácida de naringina. *Actas XI Congreso Argentino de Ciencia y Tecnología de Alimentos Buenos Aires, Argentina* 1:1–7
- Scalmanian G, Frisch MJ (2010) Continuous surface charge polarizable continuum models of solvation. I. General formalism. *J Chem Phys* 132:114110
- Selvaraj S, Krishnaswamy S, Devashya V, Sethuraman S, Krishnan UM (2014a) Flavonoid-metal ion complexes: a novel class of therapeutic agents. *Med Res Rev* 34:677–702. <https://doi.org/10.1002/med.21301>
- Selvaraj S, Krishnaswamy S, Devashya V, Sethuraman S, Krishnan UM (2014b) Investigations on the membrane interactions of naringin and its complexes with copper and iron: implications for their cytotoxicity. *RSC Adv* 4:46407–46417. <https://doi.org/10.1039/C4RA08157A>
- Sheldrick G (2008) A short history of SHELX. *Acta Crystallogr Sect A* 64:112–122. <https://doi.org/10.1107/S0108767307043930>
- Sheldrick GM (2015) Crystal structure refinement with SHELXL. *Acta Crystallogr Sect C Struct Chem* 71:3–8. <https://doi.org/10.1107/S2053229614024218>
- Smith MA, Rottkamp CA, Nunomura A, Raina AK, Perry G (2000) Oxidative stress in Alzheimer's disease. *Biochim Biophys Acta Mol Basis Dis* 1502:139–144. [https://doi.org/10.1016/S0925-4439\(00\)00040-5](https://doi.org/10.1016/S0925-4439(00)00040-5)
- Spek AL (2009) Structure validation in chemical crystallography. *Acta Crystallogr Sect D Biol Crystallogr* 65:148–155. <https://doi.org/10.1107/S090744490804362X>
- Stoll S, Schweiger A (2006) EasySpin, a comprehensive software package for spectral simulation and analysis in EPR. *J Magn Reson* 178:42–55. <https://doi.org/10.1016/j.jmr.2005.08.013>
- Swarnkar G et al (2012) A naturally occurring naringenin derivative exerts potent bone anabolic effects by

- mimicking oestrogen action on osteoblasts. *Br J Pharmacol* 165:1526–1542. <https://doi.org/10.1111/j.1476-5381.2011.01637.x>
- Tamayo LV et al (2016) Copper (II) complexes with naringenin and hesperetin: cytotoxic activity against A 549 human lung adenocarcinoma cells and investigation on the mode of action. *Biomaterials* 29:39–52. <https://doi.org/10.1007/s10534-015-9894-0>
- Tan M, Zhu J, Pan Y, Chen Z, Liang H, Liu H, Wang H (2009) Synthesis, cytotoxic activity, and DNA binding properties of copper (II) complexes with hesperetin, naringenin, and apigenin. *Bioinorg Chem Appl*. <https://doi.org/10.1155/2009/347872>
- Uivarosi V, Badea M, Rodica O, Velescu B, Aldea V (2016) Synthesis and characterization of a new complex of oxovanadium (IV) with naringenin, as potential insulinomimetic agent. *Farmacia* 64:175–180
- Unsalan O, Erdogan Y, Gulluoglu MT (2009) FT-Raman and FT-IR spectral and quantum chemical studies on some flavonoid derivatives: baicalein and Naringenin. *J Raman Spectrosc* 40:562–570. <https://doi.org/10.1002/jrs.2166>
- Valko M, Rhodes CJ, Moncol J, Izakovic M, Mazur M (2006) Free radicals, metals and antioxidants in oxidative stress-induced cancer. *Chem Biol Interact* 160:1–40. <https://doi.org/10.1016/j.cbi.2005.12.009>
- Wang H-L, Yang Z-Y, B-d Wang (2006) Synthesis, characterization and the antioxidative activity of copper (II), zinc (II) and nickel (II) complexes with naringenin. *Trans Met Chem* 31(4):470–474
- Waris G, Ahsan H (2006) Reactive oxygen species: role in the development of cancer and various chronic conditions. *J Carcinog* 5:14–14. <https://doi.org/10.1186/1477-3163-5-14>

Publisher's Note Springer Nature remains neutral with regard to jurisdictional claims in published maps and institutional affiliations.